Topological Transitions of Fast Ion Orbits in Toroidal Plasmas

L.-G. Eriksson, F. Porcelli*, and I. Furno*

JET Joint Undertaking, Abingdon, Oxfordshire, OX14 3EA, U.K.

* Dipartimento di Energetica, Politecnico di Torino, Italy.

INTRODUCTION.

The question of confinement of supra thermal ions in the MeV range and their influence on the stability is of great importance for magnetically confined plasmas. In order to assess these issues a detailed knowledge of the distribution function of the fast ions is needed. Here we study the distribution function of fast ions with non-standard orbits when they slow down collisionally. In particular, we focus on ions which have trajectories in phase space that intersect the locus of so-called pinch orbits (a generalisation of the trapped passing boundary). As the ions cross the pinch locus their orbits undergo topological transitions.

We refer to orbits as non-standard when the radial excursion of the guiding centre cannot be assumed to small compared to the distance between a point along the orbit and the magnetic axis. In fact, as discussed in Ref.[1], the standard treatment of trapped particle orbits breaks down in the central plasma region of radius $\delta_p \equiv \Delta^{2/3} R$, where $\Delta \equiv 2q\rho / R$, ρ is the average ion Larmor radius, R is the major toroidal radius, $q(r) \approx rB_\varphi / RB_\vartheta$ is the winding index of the magnetic field lines, B_φ and B_ϑ are the toroidal and poloidal magnetic field components, respectively. For example, for a $1MeV$ hydrogen ion and typical parameters of the JET Tokamak, $\delta_p \sim 0.3m$ is about one third of the plasma minor radius. In the absence of collisions, the orbit equation for the particle guiding centres can be obtained from the invariance of the particle kinetic energy, $E = mv^2 / 2$, magnetic moment, $\mu = mv_\perp^2 / 2B$, and canonical toroidal momentum, $P_\varphi = (Ze / c)\psi - mRv_\parallel B_\varphi / B$, where $\psi \geq 0$ is the poloidal magnetic flux. Let us introduce the dimensionless variables $\hat{r} \equiv r / \delta_p$, $\hat{\lambda} \equiv (R / \delta_p)\lambda$, $\hat{\psi} \equiv (2q_0 / B\delta_p^2)\psi$ and $\hat{\psi}_\varphi \equiv (2q_0 / B\delta_p^2)(cP_\varphi / Ze)$. In the non standard regime where $\hat{\lambda} < 1, \hat{\psi}_\varphi < 1$, the relevant Hamiltonian for the collisionless guiding centre is then given by [1],

$$H(\hat{x}, \hat{y}; \hat{\psi}_\varphi) = (\hat{x}^2 + \hat{y}^2 - \hat{\psi}_\varphi)^2 - \hat{x} = \hat{\lambda}, \tag{1}$$

where $\hat{x} = \hat{r}\cos\vartheta$, $\hat{y} = \hat{r}\sin\vartheta$ are canonically conjugate variables, with $\hat{x}$ playing the role of the of the canonical momentum and $\hat{\lambda}$ is the effective energy.

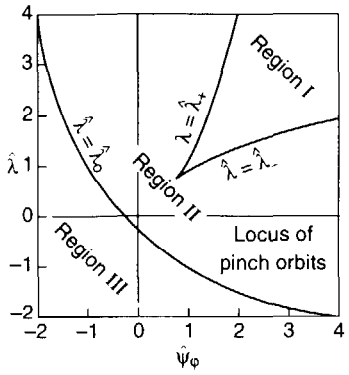

Fig. 1. Parameter plane subdivided by $\hat{\lambda} = \hat{\lambda}_0$ *and* $\hat{\lambda} = \hat{\lambda}_{\pm}$.

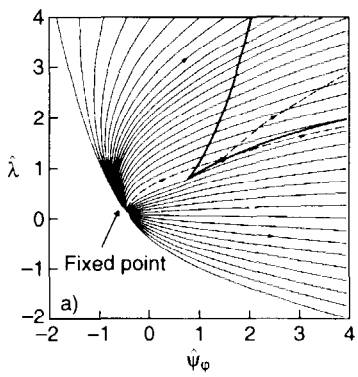

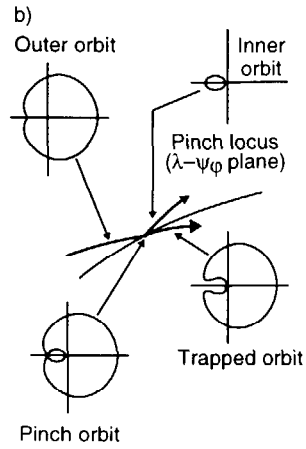

Fig. 2. (a) Characteristic curves; (b) Branching diagram.

The fixed point solutions of Hamilton's equations define three curves in the $(\hat{\lambda}, \hat{\psi}_\varphi)$ plane, represented in Fig. 1: each point within region I corresponds to two orbits, which are nested into each other; one orbit pertains to each point within region II, while no orbits exist within region III. The curves $\hat{\lambda} = \hat{\lambda}_0(\hat{\psi}_\varphi)$, $\hat{\lambda} = \hat{\lambda}_+(\hat{\psi}_\varphi)$ correspond to the locus of the co- and counter-passing stagnation orbits, where $\sigma_\parallel = \pm 1$ respectively; the separatrix curve, $\hat{\lambda} = \hat{\lambda}_-(\hat{\psi}_\varphi)$, corresponds to the locus of the (unstable) pinch orbits. A more detailed orbit classification is given in Ref. [2].

COLLISIONAL SLOWING DOWN.

As shown in Ref. [1], the orbit-averaged Fokker-Planck equation takes the form

$$\frac{dF}{d\hat{t}} = \frac{\partial F}{\partial \hat{t}} + \dot{\hat{\psi}}_\varphi \frac{\partial F}{\partial \hat{\psi}_\varphi} + \dot{\hat{\lambda}} \frac{\partial F}{\partial \hat{\lambda}} = \tau_s v^3 \langle S \rangle, \tag{2}$$

where $\hat{t} = t/\tau_s$ (τ_s is the slowing down time, which is here assumed to be constant), $F = F[\hat{t}, \hat{\psi}_\varphi(\hat{t}), \hat{\lambda}(\hat{t})] \equiv v^3 f$, and the characteristic equations are

$$\dot{\hat{\psi}}_\varphi = \langle \hat{r}^2 \rangle + \hat{\psi}_\varphi / 3, \qquad \dot{\hat{\lambda}} = 2\hat{\lambda}/3, \tag{3}$$

where $\dot{\alpha} \equiv d\alpha/d\hat{t}$ and angle brackets denote bounce averaging. The function $g(\hat{\lambda}, \hat{\psi}_\varphi, \sigma) = \langle \hat{r}^2 \rangle$ is a double-valued function of $(\hat{\lambda}, \hat{\psi}_\varphi)$ within region I of Fig. 1, hence the need to introduce an index: $\sigma = -1$ for the inner orbit and $\sigma = +1$ for the outer orbit. As shown

in Fig. 2, the characteristic curves in the $(\hat{\lambda}, \hat{\psi}_\varphi)$ plane can be thought of as originating from a fixed point at $\hat{\lambda}_f = 0$, $\hat{\psi}_{\varphi f} = -3(16)^{-2/3} \approx -0.47$ as $\hat{t} \to -\infty$. Some of the curves intersect the pinch locus. At the intersection point, a branching of the characteristic curves occurs, as represented by the diagram of Fig. 2a. An outer orbit in region I evolves into a pinch orbit. Thereafter, a small perturbation transforms the orbit, either into the adjacent inner orbit in region I, or into the adjacent *trapped* orbit in region II. A third branch, which maps the pinch locus onto itself, is dynamically unstable.

In order to determine which of the two stable branches an orbit will follow, one can use a statistical method to derive the *transition probabilities* across the locus of the pinch orbits [1]. The equations of motion are determined by the *time-dependent* Hamiltonian (1), $\hat{\lambda}(\hat{t}) = H[\hat{x}, \hat{y}, \hat{\psi}_\varphi(\hat{t})]$, where $\hat{\psi}_\varphi$ obeys Eq. (2). With reference to Fig. 3a, we identify the separatrix at a given time, $\hat{t} = \hat{t}_0$, and for given $\hat{\psi}_\varphi(\hat{t}_0)$, $\hat{\lambda} = \hat{\lambda}_-[\hat{\psi}_\varphi(\hat{t}_0)]$, nested into a higher $\hat{\lambda} = \hat{\lambda}_{out}(\hat{t}_0)$ trajectory (an outer orbit).

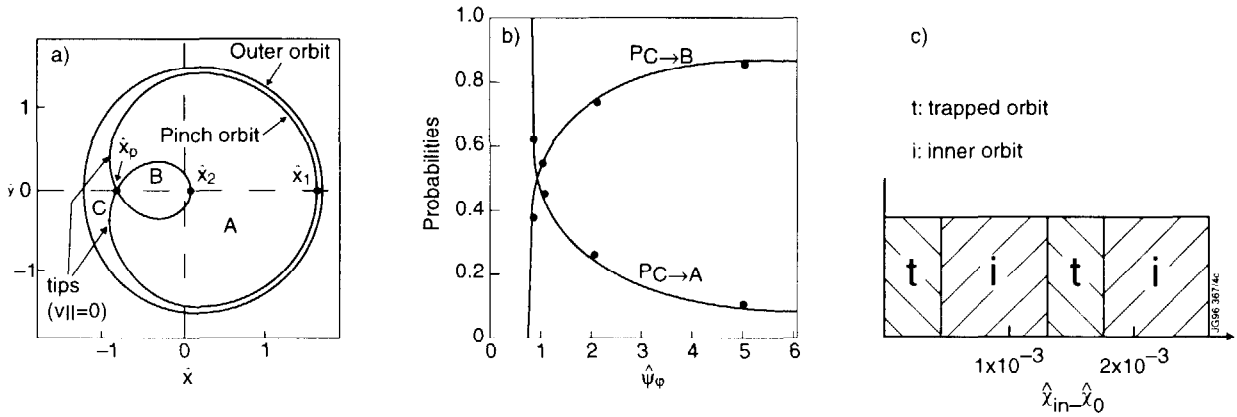

Fig 3. (a) Typical pinch and outer orbit; (b) Transition probabilities, the bullets correspond to the result of numerical simulation; (c) Band structure of $\hat{x}_{in}$.

The probability of transition from C (outer orbit) to A (trapped orbit) or B (inner orbit) is determined as the ratio of the measure, given by action integrals $\dot{I}_i = \oint_i \hat{y} d\hat{x}$; i =A;B and C, of all the trajectories moving into A or B to that of all the trajectories leaving C:

$$P_{C\to A} = -\dot{I}_A / \dot{I}_C; \quad P_{C\to B} = -\dot{I}_B / \dot{I}_C. \tag{4}$$

The time derivative of the action integrals can be performed analytically [1]. Graphs of the transition probabilities along the pinch locus are shown in Fig. 3b.

In order to check the validity of Eq (4), we have numerically integrated the equation of motion and followed particles which initially had collisionless outer orbits close to the separatrix. The initial conditions were such that $\hat{y}_{in} = 0$ and the initial effective energy $\hat{\lambda}_{in} = (\hat{x}_{in}^2 - \hat{\psi}_{\varphi in})^2 - \hat{x}_{in}$ were the same for all particles and , $\hat{\psi}_{\varphi in}(\hat{x}_{in})$, $\hat{x}_{in} > 0$ was varied. The

initial conditions were then labelled according to whether the trajectories ended up in trapped or in inner orbits in the presence of electron drag. The results of this test are summarised in Fig. 3c for $\hat{\psi}_{in} \geq \hat{\psi}_{in}(\hat{x}_0) = 2$. The relative thickness of the bands in Fig. 3c is excellent agreement with the transition probabilities of Fig. 3b, as exemplified by the numerical points (bullets) superimposed over these curves. This numerical test clarifies the meaning of the transition probabilities, as representing the relative number of initial conditions evolving into trapped or outer orbits, for particles with equal initial effective energy $\hat{\lambda}_{in}$, assuming a uniform distribution of these initial conditions. For a more detailed account of the transition probabilities reported here see Ref. [1].

INFLUENCE OF PITCH ANGLE SCATTERING.

The influence of pitch angle scattering on the transition probabilities has been studied by integrating the equation of motion numerically and frequently applying a Monte Carlo operator. The Monte Carlo operator is given by [3]: $\Delta\xi = -\xi\Delta t / \tau_D \pm \sqrt{(1-\xi^2)\Delta t / \tau_D}$, where $\xi = v_\parallel / v$, τ_D is the characteristic deflection time for pitch angle scattering and $\pm$ indicates a random sign. In Fig. 4 the time evolution of λ and $\lambda_-(v, P_\varphi)$ (the pinch locus) for typical cases are shown. Fig. 4a shows the evolution of λ and λ_- without pitch angle scattering for a particle which ends up on an inner orbit; Fig. 4b shows the evolution of λ and λ_- without pitch angle scattering for a particle which ends up on a trapped orbit, and the evolution when pitch angle scattering has been added. The sharp changes of λ, λ_- (λ is of course constant in the absence of pitch angle scattering) occur near the mid-plane on the outer part of the orbit where $|\xi|$ has its maximum. With reference to the band structure discussed at the end of the previous section, variation of the initial condition $\hat{\psi}_{in}$ leads to a variation of λ_- at the starting point. The λ_--thickness, $(\Delta\lambda)_{band}$, of two neighbouring bands when slowing down only is considered corresponds to the change in λ_- over a bounce time shown in Fig 4.

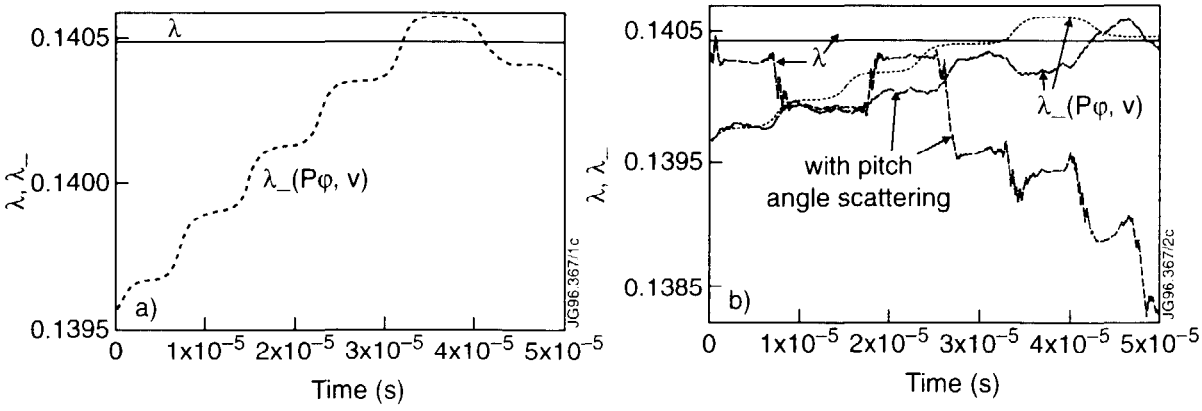

Fig 4. Time evolution of λ and λ_-; (a) a case without pitch angle scattering leading to an inner orbit; (b) a case without pitch angle scattering leading to a trapped orbit and including pitch angle scattering.

From Fig. 4 it is clear that the transition probabilities derived here are valid only if the change in λ due to pitch angle scattering over a bounce time, $(\Delta\lambda)_{p.a.s.}$, is much smaller than $(\Delta\lambda)_{band}$.

By using the fact that the change in λ occur mainly during approximately a quarter of the bounce period when the local pitch angle is near its maximum, ξ_m, we can estimate the change in λ due to pitch angle scattering as,

$$\left|(\Delta\lambda)_{p.a.s}\right| \sim \left|\frac{\partial\lambda}{\partial\xi}\right|_{\xi=\xi_m} \sqrt{\frac{\tau_b}{4\tau_D}} \approx |\xi_m| \sqrt{\frac{\tau_b}{\tau_D}}. \tag{5}$$

Now, $(\Delta\lambda)_{band} = (\partial\lambda_- / \partial P_\varphi)\Delta P_\varphi + (\partial\lambda_- / \partial \mathrm{v})\Delta \mathrm{v}$, where $\Delta P_\varphi \sim mR\xi_m \mathrm{v}\tau_b / (4\tau_s)$ and $\Delta \mathrm{v} \sim -\mathrm{v}\tau_b / \tau_s$ are the changes of P_φ and v over an orbit due to slowing down. Using the relation: $\partial\hat{\lambda}_- / \partial\hat{\psi}_\varphi = 1/(2\hat{x}_p)$ ($\hat{x}_p$ is the pinch point, see Fig 3a), and estimating $\hat{x}_p \sim 1$, we obtain

$$\left|(\Delta\lambda)_{band}\right| \sim |\xi_m| q_0 \frac{\rho}{\delta_p} \frac{\tau_b}{\tau_s}, \tag{6}$$

where ρ is the toroidal Larmor radius. Equations (5) and (6) agree well with the numerical curves in Fig. 4. With the ordering $\xi_m \sim (\delta_p / r)^{1/2}$, the condition $|(\Delta\lambda)_{p.a.s}| << |(\Delta\lambda)_{band}|$ can now be expressed as

$$\tau_D >> \tau_s \left(\frac{\tau_s}{\tau_b}\right)\left[\frac{\delta_p}{q_0\rho}\right]^2. \tag{7}$$

Eq. (7) turns out to be a quite severe constraint on τ_D. The transition probabilities derived here are therefore only valid for very cold plasmas and/or very energetic ions.

When pitch angle scattering is dominating, the following boundary conditions across the pinch locus apply: the distribution function is continuous, i.e. $f_o = f_i = f_t$, where $f_{i,o,t}$ denotes the distribution function just outside the pinch locus for the outer, inner and trapped regions respectively; furthermore, since no accumulation in the boundary layer is expected, the particle flow between the regions has to be continuous, i.e. $(\vec{j}_o + \vec{j}_t)\cdot\hat{n} = \vec{j}_i \cdot \hat{n}$, where $\vec{j}_{o,i,t}$ are the particle fluxes in phase space just outside the pinch locus for the outer, inner and trapped regions respectively, and $\hat{n}$ is a unit vector normal to the pinch locus. These three conditions together with conditions at the boundaries of phase space are sufficient to determine uniquely the solution of the distribution function. Thus, unlike the case without pitch angle scattering, no condition related to the dynamics in the transition region is necessary!

CONCLUSIONS.

In the limit of weak pitch angle scattering, i.e. $\tau_D >> (\tau_s^2 / \tau_b)(\delta_p / q_0\rho)^2$, the Fokker Planck equation reduces to a first order differential equation which can be studied by the method of characteristics. A statistical method which predicts the orbit evolution across the branch points of the characteristic curves has been developed. In the opposite limit, i.e. in the limit of strong pitch angle scattering, the evolution across the pinch locus is completely determined by the facts that the distribution function is continuos across the pinch locus and that the particle flux must be conserved.

REFERENCES

[1] F. Porcelli, L.-G. Eriksson and I Furno, Physics Letters A 216, 289 (1996).

[2] F. Porcelli, L.-G. Eriksson and H.L. Berk, in Proc. 21st EPS Conference on Contr. Fusion and Plasma Physics (Montpellier, 1994), Vol. II, p. 648.

[3] A.H. Boozer, G. Kuo-Petravic, Phys. Fluids 24, 851 (1981).